THE ASTROPHYSICAL JOURNAL, 473:1118–1124, 1996 December 20

THE ROTATIONAL SPECTRUM OF SH AND SD[1]

E. KLISCH, TH. KLAUS, S. P. BELOV,[2] A. DOLGNER, R. SCHIEDER, AND G. WINNEWISSER
I. Physikalisches Institut, Universität zu Köln, D-50937 Köln, Germany

AND

ERIC HERBST
Departments of Physics and Astronomy, Ohio State University, Columbus, OH 43210-1106
Received 1996 February 12; accepted 1996 July 9

ABSTRACT

With the Cologne terahertz spectrometer, the lower J rotational spectrum of the SD radical has been detected for the first time in the laboratory, in analogy with our previous recent detection of the SH radical. The radicals were produced by discharging H_2S (D_2S) buffered with He and H_2 (D_2). The spectra were analyzed employing Hund's case (a) coupling scheme. The SH radical has an inverted $^2\Pi$ state, as does OH, so that the $^2\Pi_{3/2}$ state is the energetically lower one. For both SH and SD, the rotational and centrifugal distortion constants, the spin orbit, the spin rotation, the Λ-doublet, and the hyperfine interaction constants were determined by combining the newly acquired experimental data with those available in the literature. The rotational constant B_0 for SD is 146885.297 (26) MHz, while our latest value for SH is 283587.62 (12) MHz (the values in parentheses denote the calculated uncertainty obtained by a least-squares fit). The SH radical and its deuterated isotopomer may be detectable in interstellar space because of the high cosmic abundance of elemental sulfur and the high abundance of H_2S. Since the $^2\Pi_{1/2}$ electronic state lies nearly 400 cm^{-1} above the $^2\Pi_{3/2}$ state, the rotational transitions in the $^2\Pi_{1/2}$ state should only be detectable in hot interstellar sources, and they are potentially good indicators of star formation.

Subject headings: line: identification — methods: laboratory — molecular data

1. INTRODUCTION

In a series of papers published in *Zeitschrift für Physik*, Hund (1933) developed a vector model for diatomic molecules to treat the interaction of the various angular momenta arising from the end-over-end rotational and electronic motions. Now known in the literature as the Hund's coupling cases, the different coupling schemes are described in five ideal cases, labeled (a) through (e) (Herzberg 1965; Townes & Schawlow 1955; Gordy & Cook 1984).

Heavier hydrides such as SH in Π or Δ states approximate closely Hund's coupling case (a), where the electronic orbital angular momentum $\boldsymbol{L}$ and the electronic spin $\boldsymbol{S}$ couple to the intermolecular axis such that their projections onto the internuclear axis Λ and Σ form the resultant Ω. The total angular momentum is $\boldsymbol{J} = \boldsymbol{\Lambda} + \boldsymbol{\Sigma} + \boldsymbol{R}$, where $\boldsymbol{R}$ is the rotational angular momentum. Both $\boldsymbol{\Lambda} + \boldsymbol{\Sigma} = \boldsymbol{\Omega}$ and $\boldsymbol{R}$ precess around the resultant $\boldsymbol{J}$. However, deviations from this idealized case occur as a consequence of the interaction of the molecular rotation with the electronic motion. In particular, spin uncoupling produces two electronic states, whereas L uncoupling leads to the lifting of the Λ-degeneracy and thus to the well-known Λ-splitting, which is observed in SH and SD. Although the spectroscopic properties of the SH radical have been established by several authors (Meerts & Dymanus 1974, 1975; Davies et al. 1978; Ashworth & Brown 1992; Morino & Kawaguchi 1995; Ram et al. 1995), and although SH and SD are potential interstellar hydrides because of the high cosmic sulfur abundance (e.g., van Dishoeck 1995), the astrophysically important lower J rotational transitions have been elusive to spectroscopic investigation, both in the laboratory and in interstellar space. Early radioastronomical searches for SH via the low-frequency, but energetically high-lying, direct Λ-doublet transitions were negative (Meeks, Gordon, & Litvak 1969; Heiles & Turner 1971). For SH and SD, the pure rotational transitions occur in the shorter submillimeter wave region, which is beset with various laboratory difficulties, the most important of which rests in the limited availability of broadband tunable frequency sources. In addition, astrophysical observations are hampered severely by restricted atmospheric transmission.

Recently we detected the $J = 3/2 \leftarrow 1/2$ pure rotational transition of SH near 870 GHz in its $^2\Pi_{1/2}$ electronic state (Klisch et al. 1996). The higher J pure rotational spectrum of SH has been measured directly by the far-IR Fourier transform method (Morino & Kawaguchi 1995). We have now complemented these data with the measurement of several pure rotational transitions of SD in both the $^2\Pi_{1/2}$ and $^2\Pi_{3/2}$ electronic states, as well as in vibrationally excited states ($v \leq 4$). It is the purpose of the present paper to report the recent SH and SD measurements in the vibrational ground state, so that astronomical line searches can be undertaken for these species.

2. EXPERIMENTAL

The essential parts of the Cologne terahertz spectrometer (Winnewisser 1995) are the frequency- and phase-stabilized high-frequency, broadband tunable backward wave oscillators (BWOs) supplied by the ISTOK Research and Production Company, Moscow region, Russia (Belov et al. 1994). For the experiments reported here, the power output of the high-frequency BWO OB-82 was split twofold: a small fraction was used to drive a mixer system fed by a KVARZ frequency synthesizer in the 78–118 GHz region,

[1] This paper is dedicated to Professor Friedrich Hund on the occasion of his 100th birthday.

[2] On leave of absence from the Microwave Spectroscopy Laboratory, Institute of Applied Physics, Nizhnii Novgorod, Russia 603024.

while the major portion of the BWO radiation (typically 1–3 mW) was focused through a free space absorption cell and then detected with a magnetically tuned, He-cooled InSb hot electron bolometer, achieving enhanced sensitivity between 1–2 THz. The free space absorption cell was equipped with a DC discharge unit. For well-isolated, single, and strong lines, the measurement accuracy in the Doppler-limited mode is better than ± 5 kHz (Belov et al. 1995; Winnewisser et al. 1996). The SH and SD spectra have been measured with less accuracy, for a variety of reasons such as partial blending, baseline problems, and insufficient signal-to-noise ratio. The measurement accuracy is estimated to be typically 50 kHz for the stronger lines.

The SH rotational spectrum (Klisch et al. 1996) was detected by discharging H_2S together with H_2 and He at the total pressure of about 150 μbar. The discharge current was set between 350 and 400 mA. Simultaneously the dimer disulfane, HSSH, was observed as monitored through its $^rQ_3$ branch (Belov et al. 1994). It is interesting to note that in a discharge of pure H_2S an additional radical, HSS, has been detected recently by Yamamoto & Saito (1994) and Ashworth, Evenson, & Brown (1995). Thus, the discharge of H_2S leads to a number of reaction products, and although three have been detected now—SH, SSH, and HSSH—at present little is known about their branching ratios and how their relative abundances might depend on the detailed experimental conditions of the discharge.

The spectrum of SD was observed under similar conditions, after replacing H_2S and H_2 by D_2S and D_2, respectively. The deuterium sulfide, D_2S, was prepared by solvolysis of aluminum sulfide Al_2S_3 with deuterium oxide D_2O, according to the synthesis of deuterium bromide described by Clusius & Wolf (1947):

$$Al_2S_3 + 6\,D_2O \rightarrow 3\,D_2S + 2\,Al(OD)_3\ .$$

The aluminum sulfide was obtained from the elements in a thermal reaction (Waitkins & Shutt 1946):

$$2\,Al + 3\,S \rightarrow Al_2S_3\ .$$

3. ANALYSIS OF THE SPECTRA

The observed pure rotational spectra of SH and SD arise from two stacks of energy levels pertaining to the $^2\Pi_{1/2}$ and $^2\Pi_{3/2}$ spin-orbit split states. The ground electronic state of the radicals is an inverted $^2\Pi$ state, so that the $^2\Pi_{3/2}$ substate is the energetically lower one. The $^2\Pi_{1/2}$ substate lies nearly 400 cm^{-1} higher and, in the interstellar medium, it will only be populated in high-temperature sources. For both SH and SD, we have detected the $J = 3/2 \leftarrow 1/2$ transition for the $^2\Pi_{1/2}$ electronic state. Figure 1 shows an improved recording of this transition for SH, published originally in Klisch et al. (1996), while the analogous SD transition is displayed in Figure 2. For SD, several additional transitions in both the $^2\Pi_{1/2}$ and $^2\Pi_{3/2}$ electronic states were observed. In particular, for the $^2\Pi_{1/2}$ state, we detected the third rotational transition $J = 7/2 \leftarrow 5/2$, whereas for the $^2\Pi_{3/2}$ state the two lowest rotational transitions ($J = 5/2 \leftarrow 3/2$ and $J = 7/2 \leftarrow 5/2$) were recorded. The rotational transitions for both radicals are split by the effect of Λ-doubling by different amounts for the two electronic states, since the doubling constant q for the $^2\Pi_{3/2}$ state is smaller than the doubling constant p for the $^2\Pi_{1/2}$ state. Accordingly, for SD the measured Λ-doubling of the $J = 7/2 \leftarrow 5/2$ transition is about 100 MHz for $^2\Pi_{3/2}$, whereas for the same transition in the $^2\Pi_{1/2}$ state, it is

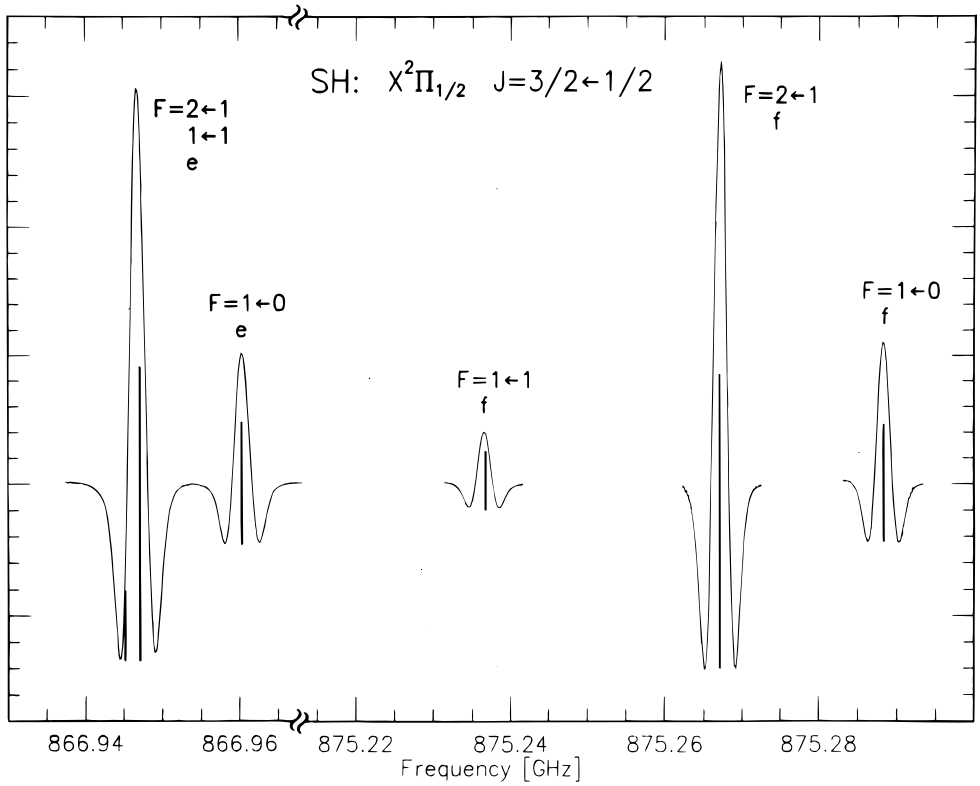

FIG. 1.—Observed line pattern of the $J = 3/2 \leftarrow 1/2$ transition of SH. The sticks indicate the relative intensities of the hyperfine components. This recording should be compared with Fig. 2 of Klisch et al. (1996). The improvement in signal-to-noise ratio between the two spectra arises from the implementation of a magnetically tuned, hot electron InSb bolometer (Belov et al. 1995).

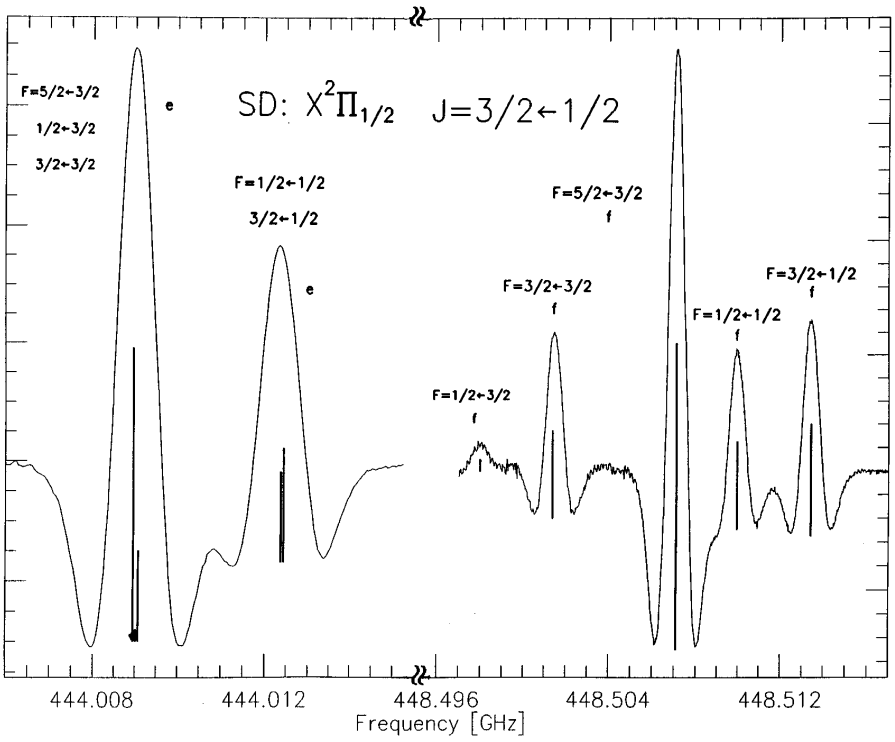

FIG. 2.—Recorded spectrum of the $J = 3/2 \leftarrow 1/2$ transition of SD in its $^2\Pi_{1/2}$ state. The hyperfine splitting is apparent. The two Λ split components with their associated hyperfine structure are displayed in different frequency scales.

over 4 GHz, as can be seen from the terahertz spectra shown in Figure 3. Hyperfine splitting has been observed for the $^2\Pi_{1/2}$ $J = 3/2 \leftarrow 1/2$ transition only.

The SH and SD rotational spectra were each fitted to an effective Hamiltonian of the form

$$H_{\text{eff}} = H_{\text{SO}} + H_{\text{SR}} + H_{\text{Rot}} + H_{\text{CD}} + H_{\Lambda\text{D}} + H_{\text{hfs}} ,$$

where the subscripts SO, SR, Rot, CD, ΛD, and hfs refer to spin-orbit, spin-rotation, rotational motion, centrifugal distortion, Λ-type doubling, and hyperfine contributions, respectively. The spectroscopic constants governing these six interactions are A (spin-orbit), γ (spin-rotation), B (rotation), D, H, etc. (centrifugal distortion), p, q, D_p, D_q(Λ-type doubling), and a, b, c, d, D_d, eQq_1, and eQq_2 (hyperfine).

3.1. SH *Spectrum*

The reported measurements of the $J = 3/2 \leftarrow 1/2$ transition were used together with the Λ-type doubling data of Meerts & Dymanus (1974, 1975) and the recent far-IR Fourier transform pure rotational transitions of Morino & Kawaguchi (1995) to determine the appropriate molecular parameters of the effective Hamiltonian. Earlier predictions based on this Hamiltonian made prior to our new observations were within 3 MHz of the measured transition frequencies and are in agreement with the recent LMR measurements and predictions (Table VII) by Ashworth & Brown (1992). For further references on the earlier work on SH, the reader is referred to Morino & Kawaguchi (1995) and Ashworth & Brown (1992).

The analysis of the first pure rotational transition of SH ($X\,^2\Pi$) including hyperfine structure is based on Hund's case (a) coupling scheme. We used parity basis functions corresponding to this coupling scheme as presented by Zare et al. (1973):

$$|\, n^2\Pi_{|\Omega|}\, vJ\pm\rangle = \frac{1}{\sqrt{2}}\,[\,|\, nvJ\Omega S\Lambda\Sigma\rangle \pm (-1)^{J-S}\,|\, nvJ(-\Omega)S(-\Lambda)(-\Sigma)\rangle] ,$$

where n and v represent different electronic and vibrational states, while Λ, Σ, and Ω, the projections of $\boldsymbol{L}$, $\boldsymbol{S}$, and $\boldsymbol{J}$ on the molecular axis, are appropriate for the Hund's case (a) representation. To consider the effect of the nuclear spin $I = \frac{1}{2}$ of the ^{1}H atom in the coupling scheme $\boldsymbol{F} = \boldsymbol{J} + \boldsymbol{I}$, where $\boldsymbol{F}$ is the total angular momentum of the radical, the parity basis functions above have to be coupled with the nuclear spin functions. Details of the individual matrix elements are given in the Appendix of Klisch et al. (1996). Hamiltonian matrix elements including all six contributions to H_{eff} have been utilized, with centrifugal distortion contributions up to J^{10}. The Hamiltonian matrix has been diagonalized numerically in a nonlinear least-squares fitting procedure to determine the spectroscopic contants.

The newly observed transitions are listed in Table 1 along with relative intensities and residuals (observed − calculated frequencies). It should be noted that the spin-orbit constant A cannot be determined from our data, and the value quoted is based on the $^2\Pi \leftarrow {}^2\Sigma_i$ band system produced by flash photolysis of H_2S and observed in the optical region by Ramsey (1952). An energy level diagram containing the relevant levels of the $^2\Pi_{1/2}$ state as split by Λ-doublet and hyperfine structure effects is shown in Figure 4, which also includes the observed transitions. The $^2\Pi_{1/2}$ state lies about 375 cm^{-1} above the $^2\Pi_{3/2}$ state, as indicated in the energy level diagram (1 THz $\approx$ 33.3 cm^{-1}). As can also be seen in Figure 4, the Λ doubling splits the rotational

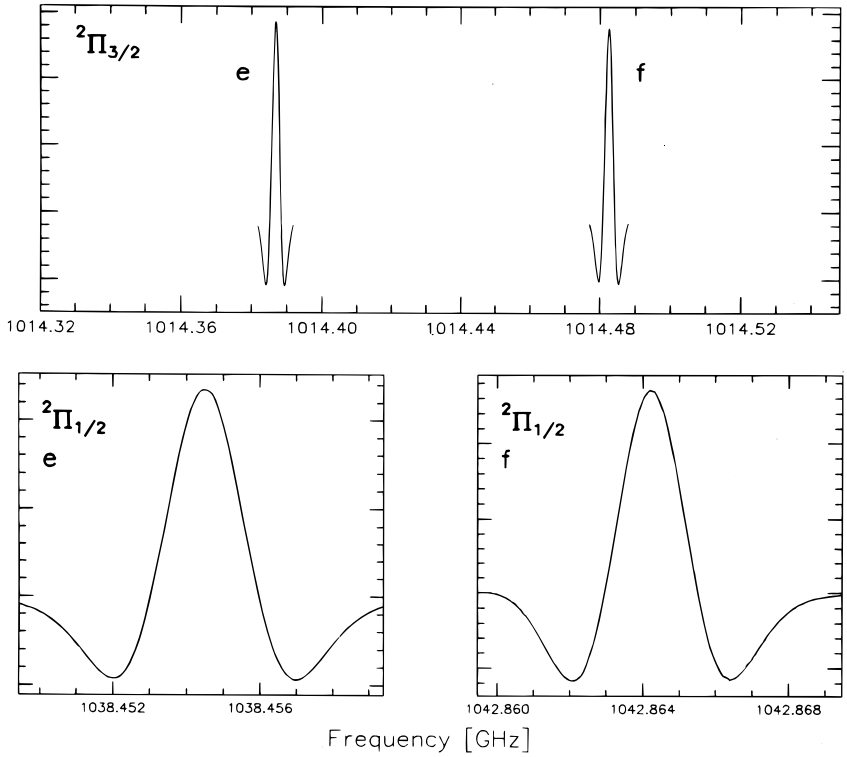

FIG. 3.—Recorded spectrum of the $J = 7/2 \leftarrow 5/2$ transition of SD. The frequency splitting of the Λ-doublet of the $^2\Pi_{3/2}$ state is about 100 MHz, whereas the $^2\Pi_{1/2}$ state has a splitting of about 4.4 GHz.

energy levels into two levels, labeled e and f; the allowed transitions here are $e \leftarrow e$ and $f \leftarrow f$. These transitions are each split into three hyperfine components with different intensities.

The spectroscopic constants obtained from the least-squares fit are shown in Table 2. The newly reported hyperfine parameters include data from the $^2\Pi_{1/2}$ state for the first time. The table also contains previous values for the constants (Morino & Kawaguchi 1995; Meerts & Dymanus 1974). It can be seen that the two sets of constants agree very well with each other. The centrifugal distortion constants L and M and magnetic hyperfine Λ-doubling constant D_d have been determined for the first time.

3.2. SD *Spectrum*

Once again, case (a) basis functions of definite parity (Zare et al. 1973) were used to determine the matrix elements, which were then employed in least-squares fitting the measured pure rotational transitions in both $^2\Pi_{1/2}$ and $^2\Pi_{3/2}$ electronic states (Klisch et al. 1996). The Meerts & Dymanus (1975) beam measurements of the direct Λ-type spectrum with associated hyperfine structure were used to supplement our data. To include the effect of the nuclear hyperfine interaction for the $I = 1$ spin of the deuterium atom, matrix elements for the electric quadrupole interaction (eQq_1, eQq_2) were needed in addition with matrix elements for the magnetic dipolar hyperfine interaction. The newly observed transitions are listed in Table 3 along with relative intensities and residuals (observed − calculated frequencies). The molecular constants determined from the nonlinear least-squares fit to the data are shown in Table 4. An energy level scheme with measured transitions of $J = 7/2 \leftarrow 5/2$ are given in Figure 5. This figure shows rotational energy levels in both spin-orbit split states but does not depict hyperfine structure.

In fitting the assorted hyperfine interactions, we determined the magnetic dipole contributions a, b, c, dD_d as well as both electric quadrupole terms eQq_1 and eQq_2. For the spin-orbit parameter A, which determines the splitting between the $^2\Pi_{1/2}$ and $^2\Pi_{3/2}$ states, we adopted the value

TABLE 1

MEASURED TRANSITION FREQUENCIES OF SH ($J = 3/2 \leftarrow 1/2$ TRANSITION) IN THE $X\,^2\Pi_{1/2}$ STATE

J'	F'	Ω'	Symmetry	←	J''	F''	Ω''	Symmetry′	ν (MHz)	Relative Intensity	Observed − Calculated (MHz)
1.5	1.0	0.5	e		0.5	1.0	0.5	e	866946.734 (100)	0.125	+0.116
1.5	2.0	0.5	e		0.5	1.0	0.5	e	866946.734 (50)	0.625	−0.375
1.5	1.0	0.5	e		0.5	0.0	0.5	e	866960.317 (80)	0.250	−0.065
1.5	1.0	0.5	f		0.5	1.0	0.5	f	875236.537 (100)	0.125	−0.209
1.5	2.0	0.5	f		0.5	1.0	0.5	f	875267.136 (50)	0.625	−0.068
1.5	1.0	0.5	f		0.5	0.0	0.5	f	875288.347 (80)	0.250	+0156

NOTE.—Numbers in parentheses denote the estimated uncertainties of measured frequencies in units of the last quoted digit. Uncertainties are 1 σ.

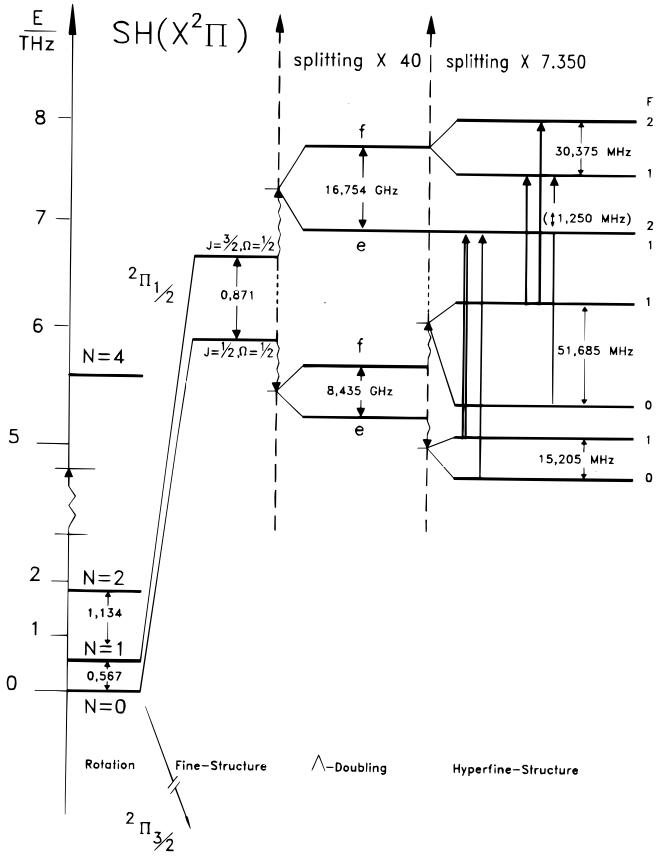

FIG. 4.—Energy level of SH. The "pure" rotational ladder has been included on the left (Hund's case [b]). The effect of fine structure, Λ-doubling, and hyperfine structure is displayed for the $^2\Pi_{1/2}$ state that is energetically 375 cm^{-1} above the $^2\Pi_{3/2}$ state, which is indicated. The observed $J = 3/2 \leftarrow 1/2$ transitions are indicated by bold arrows.

quoted by Zeitz et al. (1985), which is based on the measurements of Ramsey (1952). For SD (as well as for SH), the spin-rotation interaction γ could be fitted with significant accuracy. In this case, γ does not represent a contribution to the fine structure, which for $^2\Pi$ electronic states is dominated by the spin-orbit interaction constant A, but is instead for low J a manifestation of an off-diagonal spin-orbit term between the $^2\Pi$ and $^2\Sigma$ states. It causes for each of the two Λ-split levels a different energy shift and thus a contribution to the transition frequencies.

TABLE 2

ELECTRONIC GROUND-STATE ROTATIONAL PARAMETERS OF SH

A. COMPARISON WITH MORINO & KAWAGUCHI

Parameter	This Work	Morino & Kawaguchi
A (THz).....	−11.297139[a]	−11.297139
γ (GHz).....	−4.5731 (44)	−4.5730 (66)
D_γ (kHz).....	460 (15)	456 (25)
B (MHz).....	283587.62 (12)	283616.89 (24)
D (MHz).....	14.4944 (33)	14.5091 (25)
H (Hz).....	194 (49)	438.3 (78)
L (Hz).....	−1.55 (32)	...
M (mHz).....	−3.32 (74)	...
p (GHz).....	9.00831 (44)	9.007048 (57)
D_p (MHz).....	−0.945 (14)	−1.067 (36)
H_p (Hz).....	−468 (66)	−440 (170)
q (MHz).....	−286.1644 (68)	−284.5189 (93)
D_q (kHz).....	56.67 (20)	56.60 (51)
H_q (Hz).....	−13.5 (22)	−12.8 (48)

B. COMPARISON WITH MEERTS & DYMANUS

Parameter	This Work	Meerts & Dymanus
a (MHz).....	33.63 (31)	32.58 (7)
b (MHz).....	−63.417 (35)	−63.44 (4)
c (MHz).....	30.32 (62)	32.44 (14)
d (MHz).....	27.36 (20)	27.36 (12)
D_d (kHz).....	54 (11)	...

[a] Fixed to the value quoted by Ashworth & Brown 1992 based on a reanalysis of the data given by Ramsey 1952.

4. INTERSTELLAR IMPLICATIONS

Although SH has not yet been detected in space, the abundance of this radical in assorted interstellar sources has been considered by a variety of modellers (Millar & Herbst 1990; Mitchell 1984; Leen & Graff 1988; Pineau des Forêts et al. 1993; Sternberg & Dalgarno 1995; Lee, Bettens, & Herbst 1996). In quiescent dense interstellar clouds, characterized by a temperature $T \approx 10$–50 K and a gas density $n \approx 10^3$–10^5 cm^{-3} at which the gas is overwhelmingly H_2, the chemistry is dominated by exothermic ion-molecule and ion-electron dissociative recombination reactions (Herbst 1995). In these sources, the calculated fractional abundance of SH is $\approx 10^{-10}$ to 10^{-12} depending on cloud

TABLE 3

MEASURED TRANSITION FREQUENCIES OF SD IN THE $X\ ^2\Pi$ STATE

J'	F'	Ω'	Symmetry	←	J''	F''	Ω''	Symmetry′	ν (MHz)	Relative Intensity	Observed − Calculated (MHz)
1.5	2.5	0.5	e		0.5	1.5	0.5	e	444009.014 (50)	0.500	+0.031
1.5	1.5	0.5	e		0.5	0.5	0.5	e	444012.349 (100)	0.185	−0.121
1.5	0.5	0.5	f		0.5	1.5	0.5	f	448498.041 (150)	0.019	−0.048
1.5	1.5	0.5	f		0.5	1.5	0.5	f	448501.451 (100)	0.148	−0.070
1.5	2.5	0.5	f		0.5	1.5	0.5	f	448507.101 (50)	0.500	+0.009
1.5	0.5	0.5	f		0.5	0.5	0.5	f	448509.935 (80)	0.148	−0.004
1.5	1.5	0.5	f		0.5	0.5	0.5	f	448513.413 (80)	0.185	+0.042
3.5	...	0.5	e		2.5	...	0.5	e	1038454.580 (100)	...	−0.009
3.5	...	0.5	f		2.5	...	0.5	f	1042864.272 (100)	...	+0.001
2.5	...	1.5	e		1.5	...	1.5	e	724773.995 (100)	...	+0.119
2.5	...	1.5	f		1.5	...	1.5	f	724822.098 (100)	...	−0.121
3.5	...	1.5	e		2.5	...	1.5	e	1014386.719 (100)	...	+0.041
3.5	...	1.5	f		2.5	...	1.5	f	1014482.557 (100)	...	−0.034

NOTE.—For frequencies that could not be resolved in hyperfine structure, the quantum numbers F and F', and the relative intensities are omitted.

TABLE 4

ELECTRONIC GROUND-STATE ROTATIONAL PARAMETERS OF SD

Parameter	Frequency
A (THz)	−11.293540[a]
γ (GHz)	−2.4253 (14)
B (MHz)	146885.297 (26)
D (MHz)	3.8804 (31)
p (GHz)	4.668406 (64)
D_p (kHz)	−293.7 (74)
q (MHz)	−76.43154 (84)
D_q (kHz)	7.657 (51)
a (MHz)	5.145 (27)
b (MHz)	−9.6355 (91)
c (MHz)	4.710 (53)
d (MHz)	4.242 (38)
eQq_1 (kHz)	148.6 (10)
eQq_2 (kHz)	−46.8 (79)

[a] Fixed to the value given by Zeitz et al. 1985.

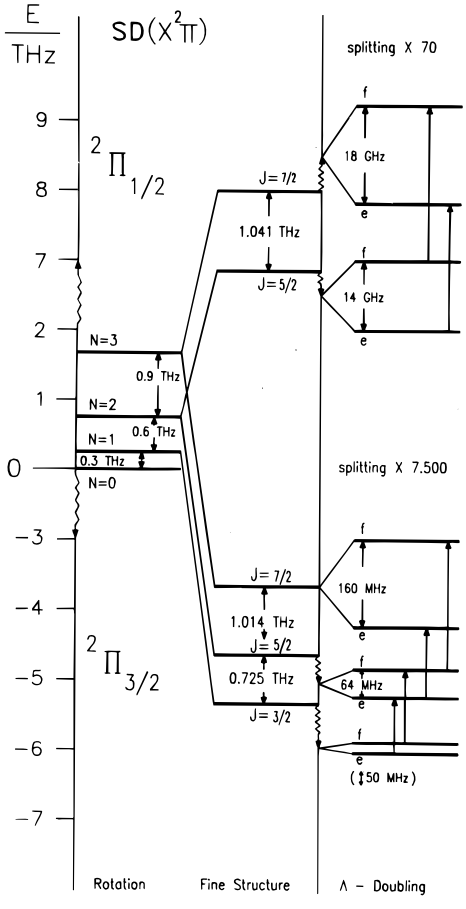

FIG. 5.—Energy level diagram of SD. The pure rotational ladder has been included on the left (Hund's case [b]). The effects of fine structure and Λ-doubling are displayed for both electronic states, $^2\Pi_{3/2}$ and $^2\Pi_{1/2}$, the latter state lying 388 cm^{-1} above the $^2\Pi_{3/2}$ state. Measured Λ-doublets of the $J = 7/2 \leftarrow 5/2$ transition are indicated by bold arrows.

density and age (Lee et al. 1996). The relatively low abundance compared with OH occurs because the "natural," exothermic ion-molecule reactions leading to the precursor ion H_2S^+,

$$S^+ + H_2 \rightarrow SH^+ + H\,,$$
$$SH^+ + H_2 \rightarrow H_2S^+ + H\,,$$

are endothermic by ≈ 1 eV (Pineau des Forêts et al. 1993). In place of these endothermic reactions, only two very slow radiative association reactions that require an electronic spin flip can produce the precursor ions H_2S^+ and H_3S^+, which lead to the SH radical via dissociative recombination:

$$S^+ + H_2 \rightarrow H_2S^+ + h\nu\,,$$
$$SH^+ + H_2 \rightarrow H_3S^+ + h\nu\,,$$
$$H_2S^+ + e \rightarrow SH + H\,,$$
$$H_3S^+ + e \rightarrow SH + H_2\,.$$

Under very high temperature conditions, the fractional abundance of SH is expected to increase because the endothermic ion-molecule synthesis above and an endothermic neutral-neutral synthesis,

$$S + H_2 \rightarrow SH + H\,,$$

produce SH efficiently. Very high temperatures in the interstellar medium are associated with shock waves that occur in regions of active star formation. Other sulfur-containing species have been detected at elevated abundance in shocked sources (Pineau des Forêts et al. 1993). For J-type shocks (Mitchell 1984; Leen & Graff 1988), model calculations show that the fractional SH abundance can reach values as high as 10^{-7} within 0.1 yr of the shock with a fairly rapid decline thereafter. Elevated abundances of SH might also be found in hot cores, which are warm but quiescent sources in the vicinity of high-mass star-forming areas, where the rising temperatures drive off saturated molecules from the surfaces of dust particles (Herbst 1995). One such saturated molecule is H_2S; this species is subsequently depleted via the reaction

$$H_2S + H \rightarrow SH + H_2\,,$$

leading to the transitory production of the SH radical, which is itself depleted by reaction with atomic hydrogen to form $S + H_2$. Detailed calculations for the abundance of SH that can be expected are in progress (Charnley 1996).

Finally, relatively high SH fractional abundances can be produced in photon-dominated regions (PDRs), which are warm, neutral regions adjoining H II sources and beset by a high photon flux. A recent PDR model (Sternberg & Dalgarno 1995) shows that the SH fractional abundance can peak at values greater than 10^{-10}.

The concentration of interstellar SD can be a significant fraction of SH, since SD is probably formed efficiently via the reaction

$$SH + D \rightarrow SD + H\,,$$

which is analogous to the OH + D reaction proposed by Croswell & Dalgarno (1985) to synthesize OD in the interstellar medium. Deuterium atoms are produced predominantly via the dissociative recombination of the molecular ion DCO^+ and electrons. Detailed model calculations by Millar, Bennett, & Herbst (1989) suggest via analogy with OH/OD that the SD/SH ratio can reach a similarly large

value of 0.05–0.50 at 10 K. If this analysis is correct, then SD may be detectable in the cold, dense interstellar medium despite the fact that the deuterium-to-hydrogen abundance ratio is on the order of 10^{-5}. The abundance of SD in warmer regions is highly uncertain.

5. CONCLUSION

Hydrides are thought to be the basic building blocks of interstellar chemical networks, but the simplest sulfur hydride has yet to be detected in space. To aid in this identification, we have made laboratory measurements of the lower J pure rotational spectra of SH and SD for the first time. Both SH and SD possess inverted electronic states, in which the $^2\Pi_{3/2}$ state is the energetically lower one, so that the lowest frequency rotational transitions ($J = 3/2 \leftarrow 1/2$) for SH and SD arise from the excited $^2\Pi_{1/2}$ state. These transitions occur at 870 GHz for SH and at 446 GHz for SD and can be seen only in warm sources because of the 400 cm^{-1} (600 K) excitation. The transitions are split by both Λ-doubling and hyperfine effects, so that the spectral patterns are certainly distinguishable. Since the atmospheric transmission at 870 GHz is about 20%–30% at excellent sites like Mauna Kea, Hawaii and Gornergrat, Switzerland, the SH transitions can be observed from the ground, albeit with some difficulty.

The work in Köln was supported in part by the Deutsche Forschungsgemeinschaft (DFG) via Special Grant SFB-301 and special funding from the Science Ministry of the Land Nordrhein-Westfalen. The work of S. P. B. at Köln was made possible by the DFG through grants aimed to support Eastern and Central European countries and the Republics of the former Soviet Union. G. W. and E. H. thank the Max-Planck-Gesellschaft and Alexander-von-Humboldt Stiftung for the Max Planck Research Award. E. H. acknowledges the support of NASA for the Ohio State program in laboratory astrophysics.

REFERENCES

Ashworth, S. H., & Brown, J. B. 1992, J. Mol. Spectrosc., 153, 41
Ashworth, S. H., Evenson, K. M., & Brown, J. B. 1995, J. Mol. Spectrosc., 172, 282
Belov, S. P., Lewen, F., Klaus, Th., & Winnewisser, G. 1995, J. Mol. Spectrosc., 174, 606
Belov, S. P., et al. 1994, J. Mol. Spectrosc., 166, 489
Charnley, S. B. 1996, private communication
Clusius, K., & Wolf, G. 1947, Z. Naturforsch, 2a, 495
Croswell, K., & Dalgarno, A. 1985, ApJ, 289, 618
Davies, P. B., Handy, E. K., Murray Lloyd, E. K., & Russell, D. K. 1978, Mol. Phys., 36, 1005
Gordy, W., & Cook, R. L. 1984, Microwave Molecular Spectra (New York: Wiley)
Heiles, C. E., & Turner, B. E. 1971, Astrophys. Lett., 8, 89
Herbst, E. 1995, Annu. Rev. Phys. Chem., 46, 26
Herzberg, G. 1965, Molecular Spectra and Molecular Structure I. Spectra of Diatomic Molecules (New York: Van Nostrand)
Hund, F. 1933, Handbuch der Physik, Band XXIV/1, 561
Klisch, E., Klaus, Th., Belov, S. P., Winnewisser, G., & Herbst, E. 1996, in Amazing Light, ed. R. Y. Chiao (New York: Springer), 355
Lee, H.-H., Bettens, R. P. A., & Herbst, E. 1996, A&A, in press
Leen, T. M., & Graff, M. M. 1988, ApJ, 325, 411
Meeks, M. L., Gordon, M. A., & Litvak, M. M. 1969, Science, 163, 173
Meerts, W. L., & Dymanus, A. 1974, ApJ, 187, 445
———. 1975, Canadian J. Phys., 53, 2123
Millar, T. J., Bennett, A., & Herbst, E. 1989, ApJ, 340, 906
Millar, T. J., & Herbst, E. 1990, A&A, 231, 466
Mitchell, G. F. 1984, ApJ, 287, 665
Morino, L., & Kawaguchi, K. 1995, J. Mol. Spectrosc., 170, 172
Pineau des Forêts, G., Roueff, E., Schilke, P., & Flower, D. R. 1993, MNRAS, 262, 915
Ram, R. S., Bernath, P. F., Engleman, R., & Brault, J. W., 1995, J. Mol. Spectrosc., 172, 34
Ramsey, D. A. 1952, J. Chem. Phys., 20, 1952
Sternberg, A., & Dalgarno, A. 1995, ApJS, 99, 565
Townes, C. H., & Schawlow, A. L. 1955, Microwave Spectroscopy (New York: Dover)
van Dishoeck, E. F. 1995, in The Physics and Chemistry of Interstellar Molecular Clouds, ed. G. Winnewisser & G. Pelz (Heidelberg: Springer), 225
Waitkins, G. R., & Shutt, R. 1946, Inorg. Synth., 2, 183
Winnewisser, G. 1995, Vib. Spectrosc., 8, 241
Winnewisser, G., Belov, S. P., Klaus, Th., & Urban, Š. 1996, Z. Naturforsch., 51a, 200
Yamamoto, S., & Saito, S. 1994, Canadian J. Phys., 72, 954
Zare, R. N., Schmeltekopf, A. L., Harrop, W. J., & Albritton, D. L. 1973, J. Mol. Spectrosc., 46, 37
Zeitz, D., Bohle, W., Werner, J., Hinz, A., & Urban, W. 1985, Mol. Phys., 54, 953